Near-infrared semiconductor subwavelength-wire lasers

A. H. Chin[a)]
Center for Nanotechnology, NASA Ames Research Center, Moffett Field, California 94035

S. Vaddiraju
Center for Nanotechnology, NASA Ames Research Center ,Moffett Field, California 94035 and Department of Chemical Engineering, University of Louisville, Louisville, Kentucky 40292

A. V. Maslov and C. Z. Ning[b)]
Center for Nanotechnology, NASA Ames Research Center, Moffett Field, California 94035

M. K. Sunkara
Department of Chemical Engineering, University of Louisville, Louisville, Kentucky 40292

M. Meyyappan
Center for Nanotechnology, NASA Ames Research Center, Moffett Field, California 94035

(Received 2 February 2006; accepted 24 March 2006; published online 21 April 2006)

We report near-infrared lasing in the telecommunications band in gallium antimonide semiconductor subwavelength wires. Our results open the possibility of the use of semiconductor subwavelength-wire lasers in future photonic integrated circuits for telecommunications applications. © *2006 American Institute of Physics*. [DOI: 10.1063/1.2198017]

Semiconductor subwavelength wires (SWWs) are ideal structures for lasers in photonic integrated circuits that have distinct advantages over current planar heterostructure semiconductor lasers.[1–3] SWWs are wires of subwavelength cross-sectional dimension and typically 10–100 μm in length that allow for high-density integration of optical components.[4] Because the gain medium of SWW lasers is the semiconductor material, they can cover a broad range of wavelengths depending on the SWW material. Unlike planar heterojunction laser structures, electronic confinement in semiconductor SWW lasers is provided by air or vacuum, and the choice of material for SWW lasers is also not as limited by lattice matching to a substrate as current semiconductor heterostructure lasers.[5] The strong optical confinement with electronic confinement in SWW lasers results in a large confinement factor[3,6] Γ. A large Γ leads to a more efficient laser,[3] making semiconductor SWW lasers in principle more efficient than standard heterostructure semiconductor lasers. Here we report the demonstration of near-infrared (NIR) lasing in a semiconductor SWW.

To demonstrate NIR SWW lasing, we study NIR lasing in GaSb SWWs with a cross-sectional dimension of 700–1500 nm and lengths of 10–70 μm dispersed on a sapphire substrate. Note that these GaSb SWWs are larger in cross-sectional dimension than semiconductor SWWs (nanowires, in particular[1]) that have previously demonstrated lasing, due to the longer wavelength involved here. We use GaSb as the gain medium because it has direct-band-gap NIR emission (~1520 nm at 10 K) (Ref. 7) in the telecommunications band and has been used previously in double-heterostructure lasers.[8] With the large refractive index for GaSb of $n \approx 3.8$, a GaSb SWW freestanding in air has a large Γ for a cross-sectional dimension greater than the wavelength of light in the wire, i.e., $d > \lambda/n = 408$ nm at $\lambda \approx 1550$ nm.[3,9]

A detailed description of the synthesis of the GaSb SWWs can be found elsewhere.[10] Briefly, the GaSb SWWs are synthesized using the spontaneous nucleation and growth technique demonstrated previously.[11] Pools of gallium supported on amorphous quartz substrates are employed for this purpose. Antimony is supplied through the vapor phase from a solid antimony source by using 10% hydrogen in argon as the carrier gas. The dissolution and subsequent supersaturation of the molten gallium droplets formed on the substrate with antimony lead to the multiple nucleation and growth of GaSb SWWs. The SWW growth experiments are performed at various temperatures ranging from 800 to 1050 °C. Following growth, the SWWs are removed from the growth substrate, suspended in alcohol, and dispersed onto sapphire substrates for optical characterization.

We utilize a temperature-dependent photoluminescence (PL) apparatus to study the NIR light emission properties of the GaSb SWWs. The samples are illuminated by a passively mode-locked Ti:sapphire laser (810 nm, ~150 fs pulse duration, 80 MHz repetition rate, and 1.5 W average power). The laser is directed towards the sample at normal incidence through a 25 mm focal length lens ($f/\#=1$) using a dichroic beam splitter. The dichroic beam splitter allows the PL emitted from the sample and collected by the same 25 mm focal length lens to be directed into the entrance slit of a 0.3 m grating monochromator (600 grooves/mm grating). The laser beam diameter at the sample is ~45 μm. The dispersed GaSb SWW substrates are placed in a microscope cryostat (under vacuum) to allow the temperature of the SWWs to be lowered. Low-temperature PL is observed by using a liquid nitrogen (LN_2) cooled InGaAs array detector coupled to the monochromator. Temperature-dependent PL measurements are performed using a single-element LN_2 cooled extended-InGaAs detector with an optical chopper and lock-in amplifier to reduce detector noise. The highly divergent nature of the light emission from the ends of the SWWs (Ref. 12) allows the study of NIR lasing in this configuration.

[a)]Electronic mail: achin@mail.arc.nasa.gov
[b)]Electronic mail: cning@mail.arc.nasa.gov

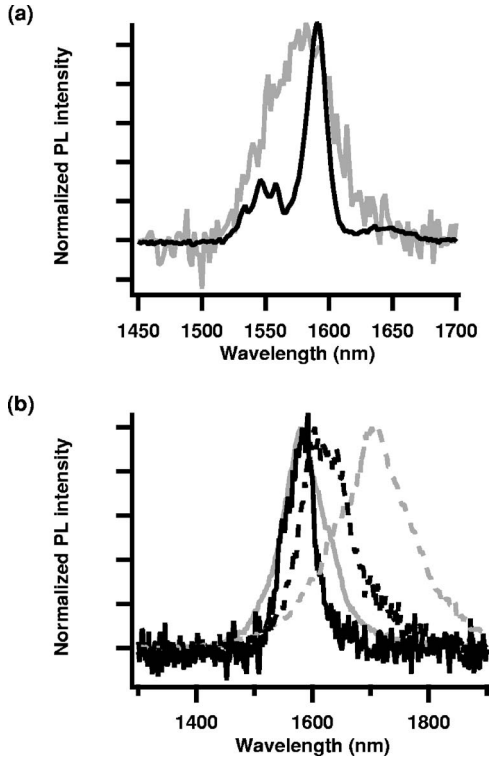

FIG. 1. GaSb SWW PL and effects of laser heating. (a) Normalized PL at 30 K of a GaSb SWW (gray) compared to a GaSb wafer (black). (b) Normalized PL of a GaSb SWW at 20 K (solid line) and 150 K (dashed line) under low (black) and high (gray) laser average power excitations, demonstrating the shift with temperature of the band gap and the effects of laser heating. Data are taken using an extended InGaAs detector with an optical chopper and lock-in amplifier.

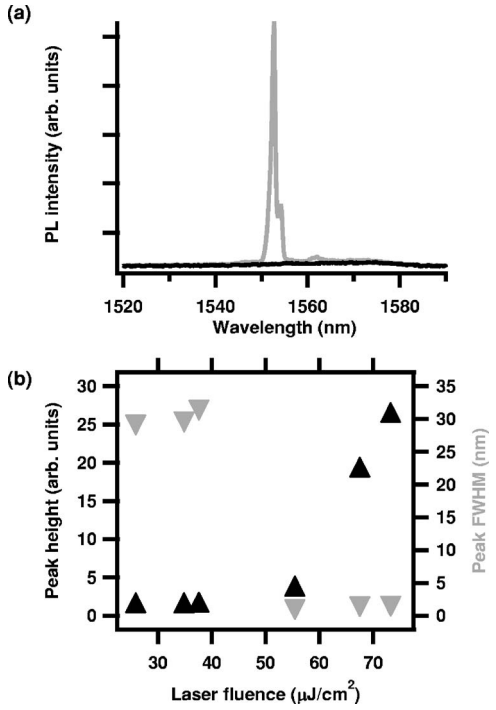

FIG. 2. GaSb SWW NIR lasing. (a) PL spectra below (black, 38 $\mu J/cm^2$) and well above threshold (gray, 73 $\mu J/cm^2$), demonstrating spectral narrowing above threshold. (b) Peak PL height at the lasing line wavelength of 1553 nm (black, up triangles) and PL width (gray, down triangles) vs laser fluence, demonstrating increased output in the lasing line and spectral narrowing to the laser linewidth above threshold. Both the PL full width at half maximum (FWHM) and peak height at each laser fluence are determined by a Gaussian fit. Data are taken at 30 K using an InGaAs array detector.

Figure 1(a) shows the PL of a single GaSb SWW compared to a GaSb wafer. The presence of multiple PL peaks in the GaSb wafer is due primarily to impurity-bound exciton emission.[7] The lack of observable features in the GaSb SWW PL may be due to line broadening from an increase in the temperature of the SWW relative to the GaSb wafer under the laser excitation. Figure 1(b) shows the shift in the peak of the PL with substrate temperature and the effect of higher laser power on the PL from a GaSb SWW. For low power excitation, the change in PL peak position with substrate temperature follows the change in band gap with temperature of bulk GaSb.[13] The consistent shift and overlap of PL emission between the SWW and the bulk confirm that the SWW is made of GaSb. With high power laser excitation, some thermal broadening occurs, but the peak position remains essentially the same when the sample is cooled to 20 K. However, at 150 K, there is clearly an effect due to laser heating. This laser heating is caused by reduced thermal transport from the SWW to the sapphire substrate which can pose a serious problem that needs to be addressed for practical SWW laser devices. Here we mitigate the problem by cooling the GaSb SWWs to cryogenic temperatures.

With high laser fluence excitation and at low temperatures (<100 K), we are able to excite GaSb SWW lasers strongly enough such that lasing can occur. Figure 2(a) shows the change in the PL spectrum for an ~ 35 μm long SWW laser at different pump laser fluences. At low fluence, the PL spectrum has a broad peak and the PL increases linearly with increasing fluence. At higher fluence, sharp peaks in the PL spectrum appear, indicating that the lasing threshold has been exceeded, and the PL peak at the primary lasing wavelength abruptly increases while the spectral width of the PL decreases. As the fluence is increased further, the primary lasing peak increases more rapidly than the spontaneous emission and the spectral width of the primary lasing line is clearly much narrower than the low-intensity PL. Figure 2(b) shows the change in the primary PL spectral width and peak height as a function of fluence, clearly showing a slope change when the lasing threshold is exceeded.

Different lasing mode spacings can be obtained by varying the diameter (transverse modes) or length (longitudinal modes) of the SWW lasers. Figure 3 shows NIR lasing behavior for GaSb SWW lasers of different lengths, demonstrating the change in mode spacing with cavity length. Due to the presence of the multiple transverse mode (~ 20 allowed modes) of the SWW lasers studied, it is difficult to identify the longitudinal modes and correlate longitudinal mode spacing to the length of the SWW.[14] However, for the data in Fig. 3(a), we can see that around threshold there are primarily four broad peaks, one of which has a narrow peak within the broad peak. We attribute the ~ 14 nm spacing between the broad peaks to the longitudinal mode spacing of the SWW. To confirm this, we can estimate the longitudinal mode spacing by using the Fabry-Pérot mode spacing relationship (approximately valid in our case, due to the relatively large waveguide cross-sectional dimension),[6] $\Delta\lambda = \lambda^2/(2nL)$, where $\Delta\lambda$ is the longitudinal mode spacing, λ is the wavelength (~ 1540 nm), n is the waveguide refractive index (~ 3.8, where the group velocity is approximately equal to the phase velocity in our case of strong confinement, neglecting both waveguide and material dispersion), and L is

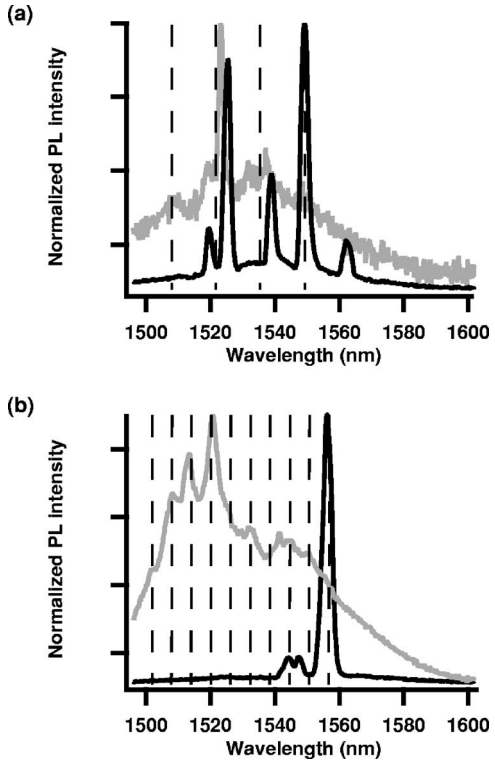

FIG. 3. SWW NIR lasing for different length GaSb SWWs. (a) Normalized PL for an ~26 μm long SWW around threshold (gray) and above threshold (black). (b) Normalized PL for an ~72 μm SWW around threshold (gray) and above threshold (black). In both panels, the dashed lines indicate the estimated position of the longitudinal modes for the dominant transverse mode. Different transverse modes will have longitudinal modes with slightly different spacings and positions. Data are taken at 20 K using an InGaAs array detector.

the waveguide length (26 μm). We estimate the longitudinal mode spacing to be ~12 nm, which is close to the observed ~14 nm spacing. For a longer SWW laser [Fig. 3(b)], we observe a smaller longitudinal mode spacing (~6 nm), and more resonances are observed around threshold within the gain bandwidth. We attribute the more closely spaced peaks within each longitudinal mode group to be due to longitudinal modes of different transverse modes.[14,15] Different modes will experience different amounts of gain, depending upon the mode confinement, reflectivity, and wavelength (position in the gain spectrum) of the mode.[3] As a result, at high excitation, the lasing peaks are spaced in a manner that does not necessarily appear to be correlated with the longitudinal mode spacing. In addition, the peaks broaden and shift to longer wavelengths with high fluence excitation, which may be attributed to heating, band gap renormalization, and carrier-induced refractive index changes.[14]

The performance of our NIR SWW lasers can be estimated by considering the carrier density at threshold. The pump fluence at the lasing threshold for the NIR SWW laser [Fig. 2(b)] is ~50 μJ/cm^2. With an absorption coefficient of $\sim 5.2\times 10^4$ cm^{-1} (~190 nm absorption depth)[7] at the excitation wavelength (810 nm), the peak carrier density is $\sim 2\times 10^{19}$ cm^{-3}. ($dN/dt=\alpha F/h\nu\tau_p$ leads to $N=\alpha F/h\nu$, where N is the carrier density, F is the fluence, α is the absorption coefficient, $h\nu$ is the photon energy, and τ_p is the laser pulse width.) Assuming an ~1000 nm diameter SWW and negligible Auger recombination, the thermalized carrier density (through carrier diffusion) is $\sim 4\times 10^{18}$ cm^{-3}, which is about two to three times the threshold carrier density in typical edge emitting double-heterostructure lasers.[6] Additional loss mechanisms due to poorly cleaved facets, surface roughness, and/or the SWW-substrate interface may be the cause of this reduced performance. Improved growth and dispersion of the GaSb SWWs will address this issue.

In summary, we have demonstrated NIR lasing in a semiconductor SWW laser. Our results are a first step towards the use of NIR semiconductor SWW lasers in photonic integrated circuits for telecommunications applications. Issues such as electrical injection and thermal transport need to be addressed before implementation of NIR SWW lasers becomes practical.

Two of the authors (A.H.C. and A.V.M.) are employed by ELORET Corporation, and their work at NASA Ames Research Center (ARC) is supported by a subcontract from the University Affiliated Research Center (UARC), operated by the University of California, Santa Cruz. The work of one of the authors (S.V.) at NASA ARC is supported by NASA-JRI-NNA05CS49A. Two of the authors (S.V. and M.K.S.) acknowledge support from the U. S. Army Space Missile Defense Command (W9113M-04-C-0024). Another author (C.Z.N.) is with UARC. Another author (A.H.C.) thanks D. S. King, H. A. Schwettman, and W. M. Pfenninger for equipment loans, and J. J. Morehead for useful discussions. The authors thank H. Partridge for his support of this project.

[1] X. Duan, Y. Huang, R. Agarwal, and C. M. Lieber, Nature (London) **421**, 241 (2003); M. H. Huang, S. Mao, and H. Feick, Science **292**, 1897 (2001).
[2] A. V. Maslov and C. Z. Ning, Appl. Phys. Lett. **83**, 1237 (2003).
[3] A. V. Maslov and C. Z. Ning, IEEE J. Quantum Electron. **40**, 1389 (2004).
[4] L. M. Tong, R. R. Gattass, J. B. Ashcom, S. L. He, J. Y. Lou, M. Y. Shen, I. Maxwell, and E. Mazur, Nature (London) **426**, 816 (2003).
[5] T. Martensson, C. P. T. Svensson, B. A. Wacaser, M. W. Larsson, W. Seifert, K. Deppert, A. Gustafsson, L. R. Wallenberg, and L. Samuelson, Nano Lett. **4**, 1987 (2004).
[6] G. P. Agrawal and N. K. Dutta, *Semiconductor Lasers*, 2nd ed. (Van Nostrand Reinhold, New York, 1993).
[7] P. S. Dutta, H. L. Bhat, and V. Kumar, J. Appl. Phys. **81**, 5821 (1997).
[8] J. P. van der Ziel, R. J. Malik, J. F. Walker, and R. M. Mikulyak, Appl. Phys. Lett. **48**, 454 (1986).
[9] L. M. Tong, J. Y. Lou, and E. Mazur, Opt. Express **12**, 1025 (2004).
[10] S. Vaddiraju, A. H. Chin, C. Z. Ning, and M. K. Sunkara (unpublished).
[11] S. Vaddiraju, A. Mohite, A. Chin, M. Meyyappan, G. Sumanasekera, B. W. Alphenaar, and M. K. Sunkara, Nano Lett. **5**, 1625 (2005).
[12] A. V. Maslov and C. Z. Ning, Opt. Lett. **29**, 572 (2004).
[13] V. Bellani, S. DiLernia, M. Geddo, G. Guizzetti, A. Bosacchi, S. Franchi, and R. Magnanini, Solid State Commun. **104**, 81 (1997).
[14] J. C. Johnson, H. Q. Yan, P. D. Yang, and R. J. Saykally, J. Phys. Chem. B **107**, 8816 (2003).
[15] P. P. Sorokin, J. D. Axe, and J. R. Lankard, J. Appl. Phys. **34**, 2553 (1963).